

REPORT DOCUMENTATION PAGE

Form Approved
OMB No. 0704-0188

Public reporting burden for this collection of information is estimated to average 1 hour per response, including the time for reviewing instructions, searching existing data sources, gathering and maintaining the data needed, and completing and reviewing the collection of information. Send comments regarding this burden estimate or any other aspect of this collection of information, including suggestions for reducing this burden, to Washington Headquarters Services, Directorate for Information Operations and Reports, 1215 Jefferson Davis Highway, Suite 1204, Arlington, VA 22202-4302, and to the Office of Management and Budget, Paperwork Reduction Project (0704-0188), Washington, DC 20503.

1. AGENCY USE ONLY (Leave blank)		2. REPORT DATE 7/16/94	3. REPORT TYPE AND DATES COVERED 6/1/91-5/31/94
4. TITLE AND SUBTITLE "Vacuum Microelectronic Devices and Their Applications Using Compound Semiconductor Technology"			5. FUNDING NUMBERS DAAL03-91-G-0161
6. AUTHOR(S) David Holcombe Wei-Nan Jiang Prof. Umesh K. Mishra			
7. PERFORMING ORGANIZATION NAME(S) AND ADDRESS(ES) University of California Department of Electrical and Computer Engineering Santa Barbara, CA 93106			8. PERFORMING ORGANIZATION REPORT NUMBER FINAL
9. SPONSORING/MONITORING AGENCY NAME(S) AND ADDRESS(ES) U. S. Army Research Office P. O. Box 12211 Research Triangle Park, NC 27709-2211			10. SPONSORING/MONITORING AGENCY REPORT NUMBER ARO 28569.2-PH
11. SUPPLEMENTARY NOTES The view, opinions and/or findings contained in this report are those of the author(s) and should not be construed as an official Department of the Army position, policy, or decision, unless so designated by other documentation.			
12a. DISTRIBUTION/AVAILABILITY STATEMENT Approved for public release; distribution unlimited.			12b. DISTRIBUTION CODE DTIC QUALITY INSPECTED 8
13. ABSTRACT (Maximum 200 words) AlGaAs/GaAs Planar-Doped-Barrier Electron Emitters: Design, Fabrication and Characterization by Wei-Nan Jiang Vacuum microelectronic devices (VMDs) are a class of devices in which electron transport occurs both in semiconductors and in vacuum. They have the potential of combining the advantages of vacuum tube based devices with those of modern semiconductor devices. The key to the success of VMDs is fabricating reliable solid state electron emitters with high emission efficiency and high emission current density. This report will present the design, growth, fabrication and characterization of Planar-Doped-Barrier Electron Emitters (PDBEEs) made of compound semiconductor AlGaAs/GaAs. In PDBEEs, electrons, as majority carriers, are injected over a triangular barrier into a high field region accelerated towards the surface. Injected Electrons gain kinetic energy from the field and lose kinetic energy through scattering processes. Those electrons with enough energy to overcome the surface barrier upon reaching the surface could be emitted into vacuum. The surface work function of semiconductors (GaAs in this work) is lowered by cesiation. An emission efficiency of 4.2 % and an emission current density of 5.8 A/cm ² have been obtained from Al _{0.3} Ga _{0.7} As/GaAs PDBEEs.			
14. SUBJECT TERMS Vacuum Microelectronic Emitters, Planar-Doped-Barrier Emitters (PDBEEs), Hot Electron Injectors			15. NUMBER OF PAGES 26
			16. PRICE CODE
17. SECURITY CLASSIFICATION OF REPORT UNCLASSIFIED	18. SECURITY CLASSIFICATION UNCLASSIFIED	19. SECURITY CLASSIFICATION OF ABSTRACT UNCLASSIFIED	20. LIMITATION OF ABSTRACT UL

19941128 154

MASTER COPY: PLEASE KEEP THIS "MEMORANDUM OF TRANSMITTAL" BLANK FOR REPRODUCTION PURPOSES. WHEN REPORTS GENERATE UNDER ARO SPONSORSHIP, FORWARD A COMPLETED COPY OF THIS FORM WITH EACH REPORT TO OUR OFFICE. THIS WILL ASSURE PROPER IDENTIFICATION.

MEMORANDUM OF TRANSMITTAL

U.S. Army Research Office
ATTN: SLCRO-IP-Library
P.O. Box 12211
Research Triangle Park, NC 27709-2211

Dear Library Technician:

☐ Reprint (15 copies) ☐ Technical Report (50 copies)
☐ Manuscript (1 copy) ☒ Final Report (50 copies)
☒ Thesis (1 copy)

☐ MS ☒ PhD ☐ Other _____

TITLE: VACUUM MICROELECTRONIC EMITTERS AND THEIR
APPLICATIONS USING COMPOUND SEMICONDUCTOR
TECHNOLOGY

is forwarded for your information.

SUBMITTED FOR PUBLICATION TO (applicable only if report is manuscript):

Sincerely,


UMESH MISHRA

DO NOT REMOVE THE LABEL BELOW
THIS IS FOR IDENTIFICATION PURPOSES

Final Report on

Vacuum Microelectronic Emitters and their Applications using Compound Semiconductor Technology

by

**David Holcombe
Wei-Nan Jiang
Prof. Umesh K. Mishra**

**ECE Department
University of California
Santa Barbara, CA. 93106**

Period of work : June 1, 1991 to May 31, 1994

Grant Number : DAAL03-91-G-0161

Accession For	
NTIS CRA&I	<input checked="checked" type="checkbox"/>
DTIC TAB	<input type="checkbox"/>
Unannounced	<input type="checkbox"/>
Justification	
By	
Distribution /	
Availability Codes	
Dist	Avail and/or Special
A-1	

Introduction

There is a great need for solid state cathodes (SSCs, or called cold cathodes) for a variety of applications, such as

- (a) vacuum microelectronic devices (VMDs) including medium power, wide bandwidth mm-wave amplifiers and high power mm-wave sources,
- (b) radiation hard systems,
- (c) planar panel displays, and
- (d) massive parallel electron beam lithography systems.

Compared to conventional thermionic cathodes, SSCs have the potential advantages of being small in size and reliable in performance. The existing SSCs can be basically divided into two groups: field emitters and planar emitters. The former, also called Spindt cathodes¹, is based on the field emission of electrons through the surface barrier (on the order of several electron-volts) under a very high field (on the order of 10^7 V/cm), which is usually realized by applying a high voltage between the anode and sharp tips. The latter is realized by generating hot electrons inside the solid state material so that the kinetic energy of electrons upon reaching the surface is higher than the surface work function. In the past two decades, extensive research has been done to fabricate field emitters and field emitter arrays (FEAs) with high emission current density. Various types of field emitters, including vertical¹ and lateral² embodiments, have been developed so far with good success. Microwave amplifiers and flat panel displays based on FEAs have also reported recently³. In the past 30 years, several types of planar emitters based on different hot electron generation mechanisms have also been reported⁴. The primary advantages of planar emitters are (i) collimated planar electron emission, (ii) ease of electron modulation and pre-bunching for high efficiency TWTs, Klystrons, etc. In order to obtain considerable emission efficiency and current density for practical applications, the surface of planar emitters is usually coated with low work function materials (on the order of one mono-layer), such as cesium and its oxide. Although the surface work function has been successfully lowered by several electron-volts, the devices with cesiated surfaces are often not stable due to the degradation of the cesiated surface.

In order to obtain electron emission from non-cesiated surfaces, it is necessary to heat electrons to energy higher than the surface work function which is usually between 4 to 5 volts for semiconductors of interest. Several structures which can generate such hot electrons have also been reported, such as Si avalanche cold cathodes (SACCs)⁵,

AlGaAs/GaAs planar-doped-barrier electron emitters (PDBEEs) ⁶, and Si MOS tunneling cathodes ⁷. However, the typical emission efficiency of SACCs and AlGaAs/GaAs PDBEEs is on the order of 10^{-5} % which is too low for practical applications. For Si MOS tunneling cathodes, although an emission efficiency of 0.7 % has been reported, the emission current was only on the order of 10^{-9} Amp. and the emission was also not stable due to the degradation of the thin oxide film under high field. In the past three years, extensive work has been done at the UCSB on the development solid state cold cathodes by using AlGaAs/GaAs planar-doped-barrier structures. An emission efficiency of over 5.0 % and an emission current density of over 5.0 A/cm^2 have been obtained from cesiated AlGaAs/GaAs PDBEEs.

In the following sections, issues concerning the carrier transport across the PDB structures and electron emission characteristics will be presented in detail. Other issues concerning the material growth of the PDB structures and device fabrication have been discussed in the attached Ph.D. thesis generated by this research.

AlGaAs/GaAs planar-doped-barrier electron emitters

A Planar-Doped-Barrier (PDB) structure basically consists of n^+ -undoped (i)- n^+ layers with a very thin p^+ layer inserted within the undoped region giving rise to a triangular barrier structure as shown in Fig. 1. Under sufficient forward bias (the channel is positively biased relative to the injector as shown in Fig. 1(c)), the acceleration region

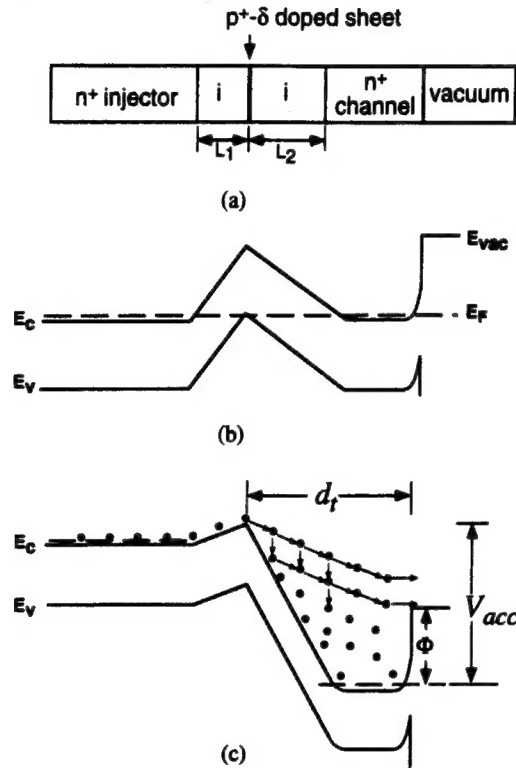


FIG. 1 Schematic diagram of a Planar-Doped-Barrier Electron Emitter showing (a) layer sequence, (b) band diagram under zero-bias, and (c) band diagram under forward bias.

(the p-i-n junction on the right of the barrier) is reversed biased and the injection region (the junction on the left) is forward biased, and electrons are injected over the triangular barrier into the high field acceleration. Injected electrons gain kinetic energy from the field and lose kinetic energy through scattering processes. The maximum kinetic energy which injected electrons can gain from the field is equal to the potential difference between the peak of the conduction band and the Fermi level of the n-type channel, the acceleration voltage qV_{acc} . Those electrons with energy larger than the surface work function upon reaching the surface could be emitted into vacuum.

Emission efficiency, defined as the ratio of emission current detected at the anode to the total bias current, is determined, assuming all emitted electrons are collected at the anode, by the electron distribution upon reaching the surface and the transmission probability for electrons crossing the surface barrier into vacuum.

The transport of electrons across the high field acceleration region and the surface channel is governed by the acceleration from the field and the relaxation through scattering. Possible scattering mechanisms involved in PDBEEs include:

- (a) optical phonon scattering,
- (b) impact ionization,
- (c) alloy scattering,
- (d) intervalley scattering,
- (e) ionized impurity scattering,
- (f) electron-electron scattering, and
- (g) coupled phonon-plasmon scattering.

Electron distribution at the surface can be known only if the scattering of hot electrons with kinetic energy of several electron-volts is fully understood. Unfortunately, studies on the transport of such hot electrons just started very recently, and experimental results of hot electron mean free path are very scattered with values between several ten to several hundred angstroms. Nevertheless, qualitatively, the larger the acceleration voltage and smaller the transit distance (d_t , defined as the distance from the peak of the barrier to the surface as shown in figure 1), the higher the concentration of electrons with energy in excess of the surface work function and hence the higher the emission efficiency.

In summary, in order to improve the emission efficiency, the acceleration voltage should be as large as possible and the transit distance (including the n^+ surface channel) should be as small as possible. This results in an extremely high acceleration field. The current flow across the barrier is therefore not necessarily governed by thermionic emission over the triangular barrier but rather by the tunneling through the band gap within the acceleration region. The thin n^+ surface channel also causes non-uniform current injection due to the current crowding effect. Both these effects degrade the emission performance of PDBEEs.

Current flow mechanisms in PDBEEs with high built-in acceleration fields

Fig. 2 shows the possible contributions to the current flow in a PDBEE under a forward bias of V_d . J_{th} is the current contribution of electrons with energy larger than the barrier height, the so called thermionic emission current. J_{tfe} is the contribution of electrons with energy less than the barrier height, the so called thermionic field emission current. J_{bb} is the contribution of electrons tunneling through the band gap of the acceleration region. J_h is the hole diffusion current. J_{ge} is the generation current within the reverse biased acceleration region (including impact ionization). J_{re} is the recombination current within the forward biased injection region. For the typical PDB structures used for emitters, the thickness of the acceleration region is very small so that J_{ge} is estimated much smaller than the thermionic emission and tunneling currents. J_h is also estimated to be neglected. Thus, the total current crossing the PDB diodes is approximately equal to

$$J_{total} \approx J_{th} + J_{tfe} + J_{bb} = J_{trans} + J_{bb}$$

where, J_{trans} is the transmission current contributed from all electrons injected from the

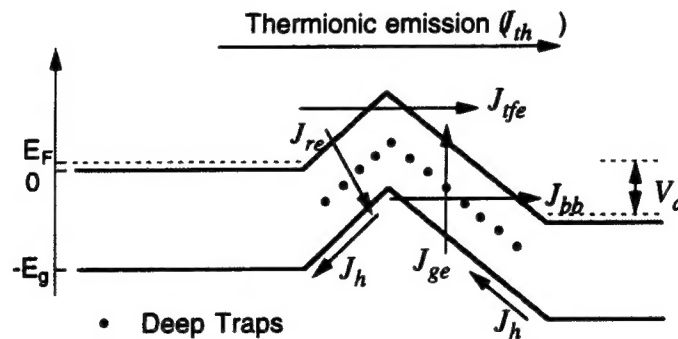


FIG. 2 Possible current flow mechanisms across the PDB structure under forward bias of V_d

injector. Fig. 3 shows the calculated current-voltage characteristics of a PDB diode. The calculation of the transmission current over the barrier is obtained by solving the quantum

mechanical transmission probability of electrons across the triangular barrier using a propagation matrix method. The tunneling current through the band gap within the acceleration region is calculated based on a modified parabolic tunneling barrier model. The inserted table shows the diode structure which has typical layer thicknesses and doping levels of a PDB electron emitter. Two important conclusions are drawn from this figure. First, the thermionic emission current is almost one order of magnitude smaller than the total transmission current, indicating the important contribution to current flow from electrons with energy less than the barrier height. Since its voltage dependence is similar to J_{th} , J_{trans} can be treated by thermionic emission theory with a smaller zero-bias barrier height. In this way, we can still terminate the region dominated by J_{trans} as the

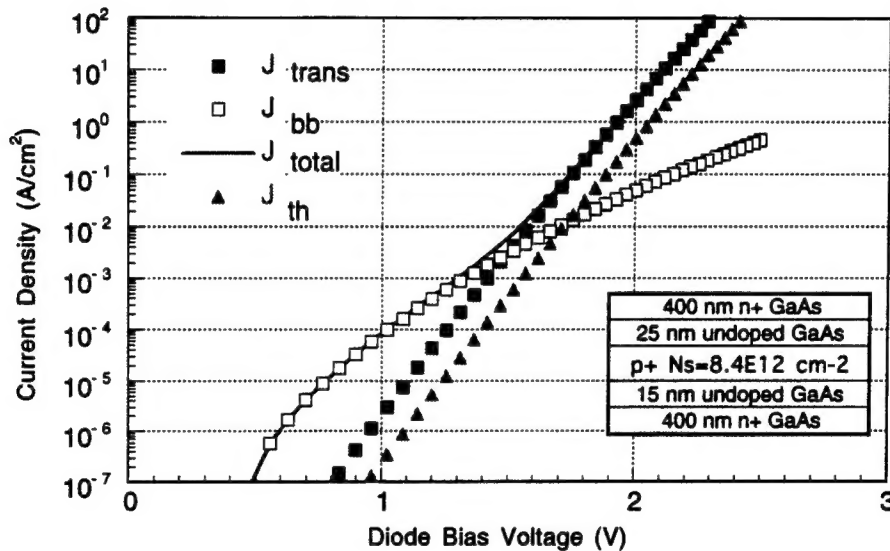


FIG. 3 Simulation I-V characteristics of a PDB diode at room temperature (300K). The current is dominated by tunneling (J_{bb}) at low bias and by transmission current (J_{trans}) at large bias. The insert is the epitaxial structure of this diode.

thermionic emission dominated region. Second, the current flow is dominated by tunneling (J_{bb}) at low bias, and dominated by the transmission current at medium and larger bias regions. For given thicknesses of the injection and acceleration regions, the cross-over bias, V_{cross} at which J_{trans} and J_{bb} intersect, increases with the doping density of the p-type layer. In Fig. 4 the calculated acceleration voltage V_{acc} for the same device is plotted as a function of the applied bias voltage (the solid line). It should be pointed out here that there is a significant deviation in the I-V characteristics at larger injection levels from the

calculated one due to the existence of a finite series resistance, and this effect is presented in Fig. 4 as the dashed line. The acceleration voltage increases with the applied bias at small and medium bias regions and saturates at large bias. Although a larger maximum acceleration voltage can be obtained by increasing the doping density of the p-type layer at a

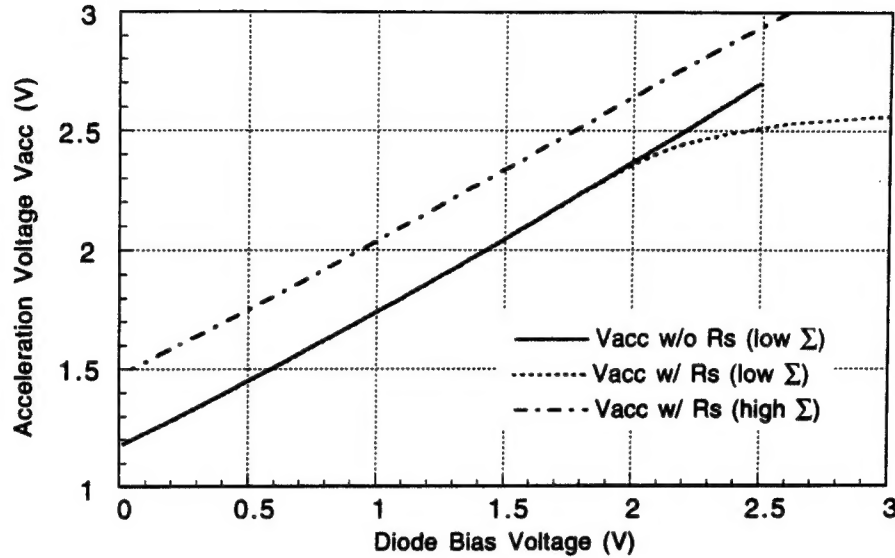


FIG. 4 Calculated acceleration voltage as a function of the bias voltage for two PDB diodes. The solid line is for the PDB diode shown in Fig. 2.7 which has a lower p+ delta doping density (Σ) without taking the series resistance into account, the dashed line is for the same diode with a series resistance, and dot-dashed line is for the diode with a higher Σ and a series resistance.

given thickness of the acceleration region (as shown the dot-dashed line in Fig. 4 which is the calculated result for a PDB diode with Σ of $1 \times 10^{13} \text{ cm}^{-2}$), the current flow is dominated by the tunneling mechanism, J_{bb} , completely before reaching the resistive region as shown in Fig. 5. Since electrons tunneling through the band gap have much lower kinetic energy gained (at least 1.4 eV lower in the case of GaAs PDB structures) from the accelerating field than those injected over the triangular barrier, the emission efficiency will be much lower if the current flow in PDBEEs is dominated by the tunneling. Therefore, it is very important to ensure that devices are operated in thermionic emission dominated region, while simultaneously having a large acceleration voltage.

Whether the current flow in a PDB structure is dominated by thermionic emission over the barrier or by the band to band tunneling can be determined experimentally by investigating the temperature dependent current-voltage (I-V) characteristics of the PDB

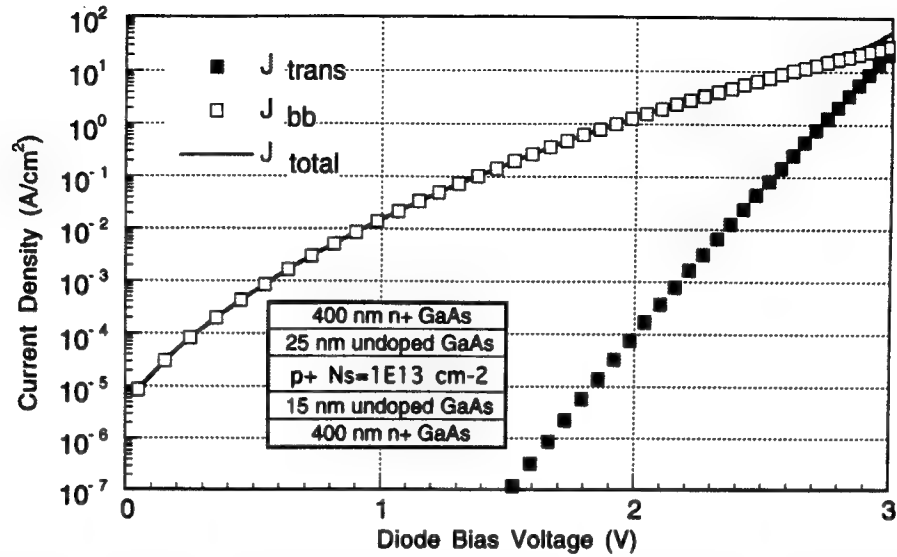


FIG. 5 Simulation I-V characteristics of a PDB diode with a higher barrier height. The current is almost completely dominated by tunneling (J_{bb}). The insert is the epitaxial structure of this diode.

diode. Fig. 6 presents the measured I-V characteristics of the PDB diode shown in Fig. 4 in the temperature range of 50 to 300 K. The theoretical simulation is also shown as symbols in the figure. Very good agreement between the simulation and experimental results indicates the validity of the model used to calculate the current flow.

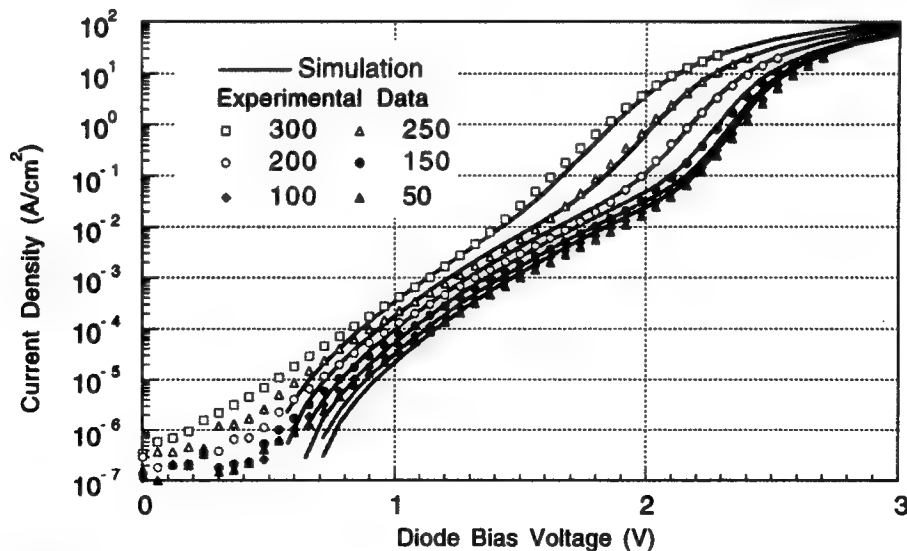


FIG. 6 Comparison between Simulated and experiments at different temperatures.

I-V curves shown in Fig. 6 can be divided into three regions: (a) a low bias region with weaker temperature dependence where the current flow is dominated by the band to band tunneling, (b) a medium bias region with stronger temperature dependence where the current flow is dominated by the thermionic emission over the barrier, and (c) a resistive region due to the existence of a certain series resistance. When the doping density of the p-type layer increases, region (a) in Fig. 6 will extend to larger bias voltage and eventually region (b) will disappear indicating the current flow is completely dominated by the band to band tunneling. On the other hand, when the doping density of the p-type layer decreases, region (b) will extend to lower bias and eventually region (a) will disappear as observed in earlier PDB diodes which had barrier heights usually less than the half of the band gap.

The ideal situation for a PDBEE is that the temperature dependent I-V characteristics should look like the one shown in Fig. 6 where a distinguished thermionic emission dominated region shows up in medium bias region and the device is operated as an emitter in this region. Fig. 7 shows the measured temperature dependent I-V characteristics of a GaAs PDBEE. By comparing it with Fig. 6, it can be easily concluded that the current flow across this GaAs PDBEE is dominated completely by the band to band tunneling which is not desired for high performance electron emitters. There are several ways to

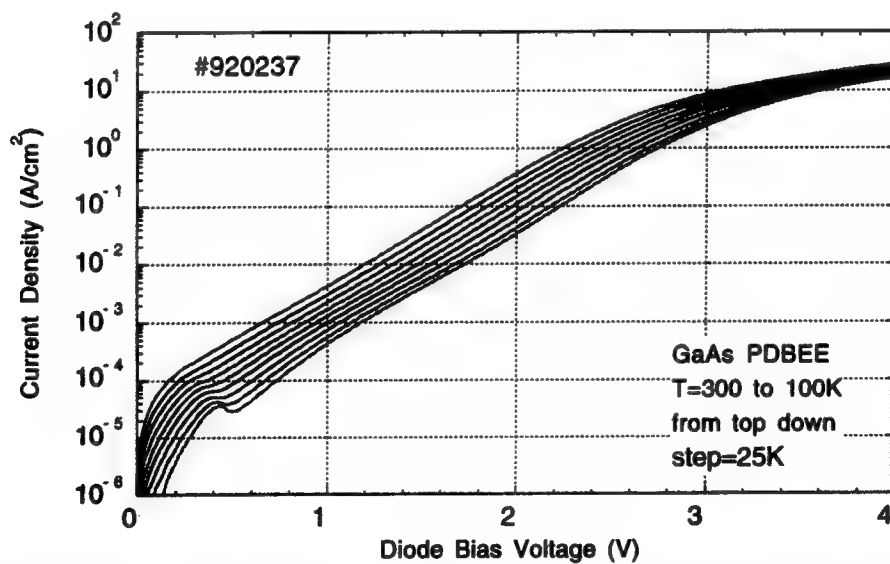


FIG. 7 Temperature dependent I-V characteristics of the GaAs PDBEE (#920237). The temperatures corresponding to the curves are from 300K to 100K from top to bottom.

suppress this tunneling relatively to the thermionic emission: (i) for given material and the thickness of the acceleration region, reducing the doping density of the p-type layer; (ii) for given material and doping density, increasing the thickness of the acceleration region; and (iii) for given doping density and the thickness of the acceleration region, choosing materials with a larger band gap.

As discussed earlier, both (i) and (ii) have some negative effects on the emission performance of PDBEEs. For method (i), although the current flow across PDB structures may be dominated by the thermionic emission, the maximum acceleration voltage is reduced. For method (ii), although a large maximum acceleration voltage can be preserved and the current flow can be dominated by thermionic emission, the transit distance and hence energy loss due to scattering is increased. The only way of suppressing band to band tunneling without sacrificing the small transit distance and large acceleration voltage is to use materials having larger band gap. $\text{Al}_{0.3}\text{Ga}_{0.7}\text{As}$ was chosen in our research because it has a larger band gap of 1.8 eV compared with 1.42 eV for GaAs, and is readily grown and doped by MBE.

Fig. 8 shows the temperature dependent I-V characteristics of the $\text{Al}_{0.3}\text{Ga}_{0.7}\text{As}$ PDBEE. By comparing with Fig. 6, it can be concluded that the current flow in medium region as region (b) indicated in the figure is dominated by the thermionic emission over the barrier.

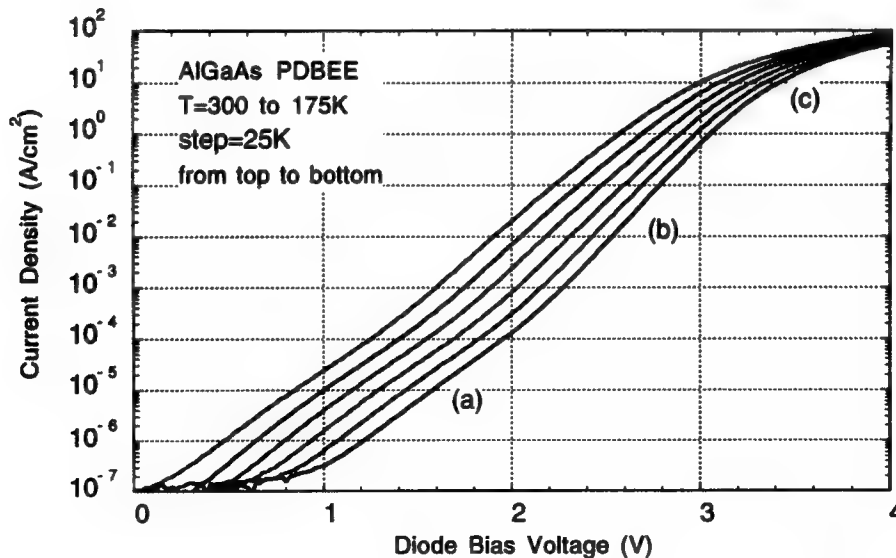


FIG. 8 Temperature dependent I-V characteristics of AlGaAs PDBEE.

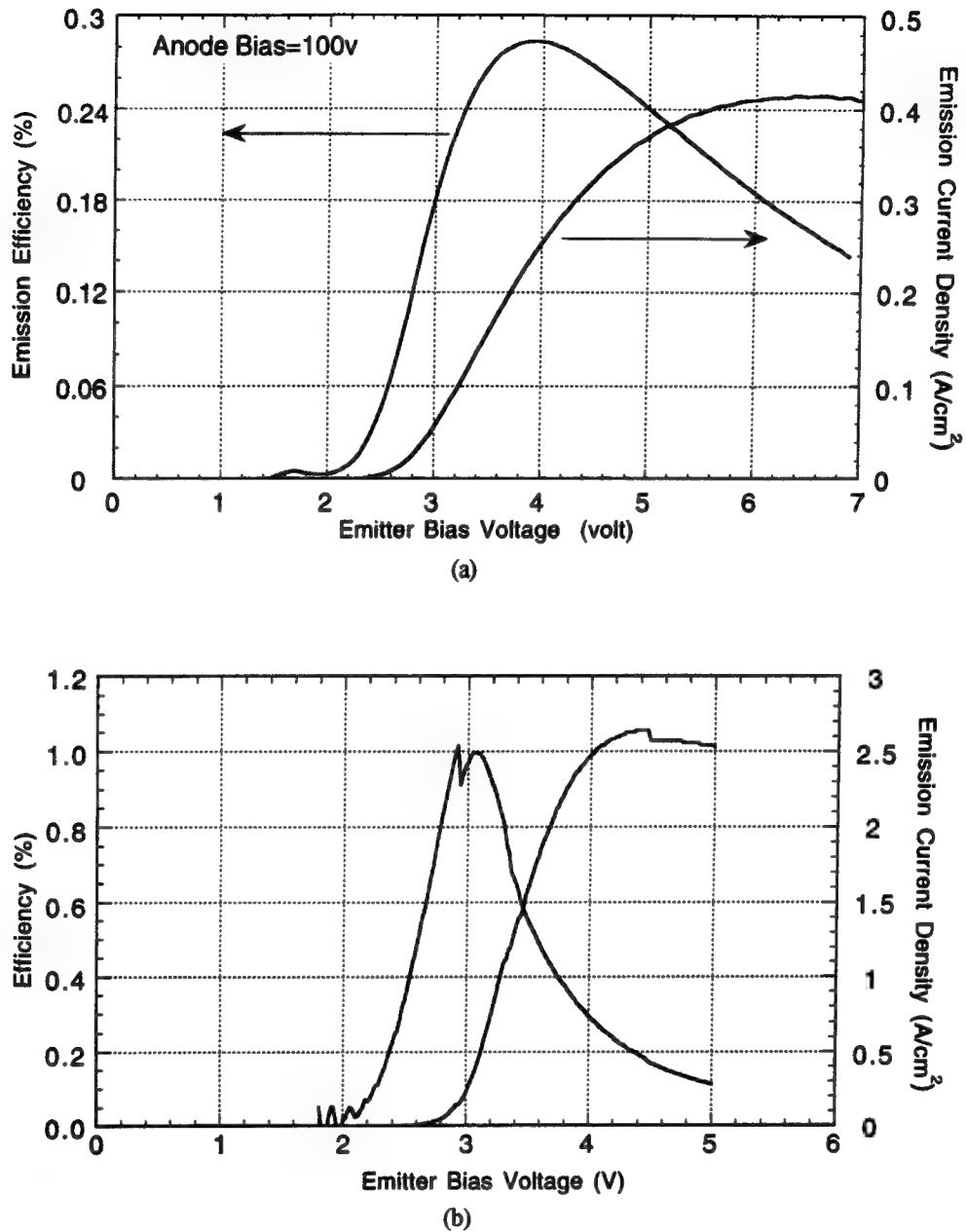


FIG. 9 Emission characteristics of a GaAs PDBEE (a), and AlGaAs PDBEE (b) showing emission efficiency and emission current density vs. emitter bias voltage. The anode bias is 100 V.

We have fabricated emitters using both GaAs and $Al_{0.3}Ga_{0.7}As$ PDB structures. Both devices have the same layer and doping structures. The only difference between them is that in the $Al_{0.3}Ga_{0.7}As$ PDBEE, the injection and acceleration regions are made of

$\text{Al}_{0.3}\text{Ga}_{0.7}\text{As}$. Temperature dependent I-V characteristics of these emitters are shown in Fig. 7 and Fig. 8. Figure 9 presents the emission current density and efficiency of the GaAs and $\text{Al}_{0.3}\text{Ga}_{0.7}\text{As}$ PDBEEs. By using $\text{Al}_{0.3}\text{Ga}_{0.7}\text{As}$ as the barrier material, the emission current density and efficiency have been improved by about 6.2 and 3.6 times.

Although the emission performance of PDBEEs can be further improved by reducing the thickness of the surface channel layer so as to reduce scattering of injected electrons, the current crowding along the thin channel decreases the effective bias voltage and hence reduces the acceleration voltage as shown in Fig. 10. Therefore, there exists a trade-off in designing the surface channel layer.

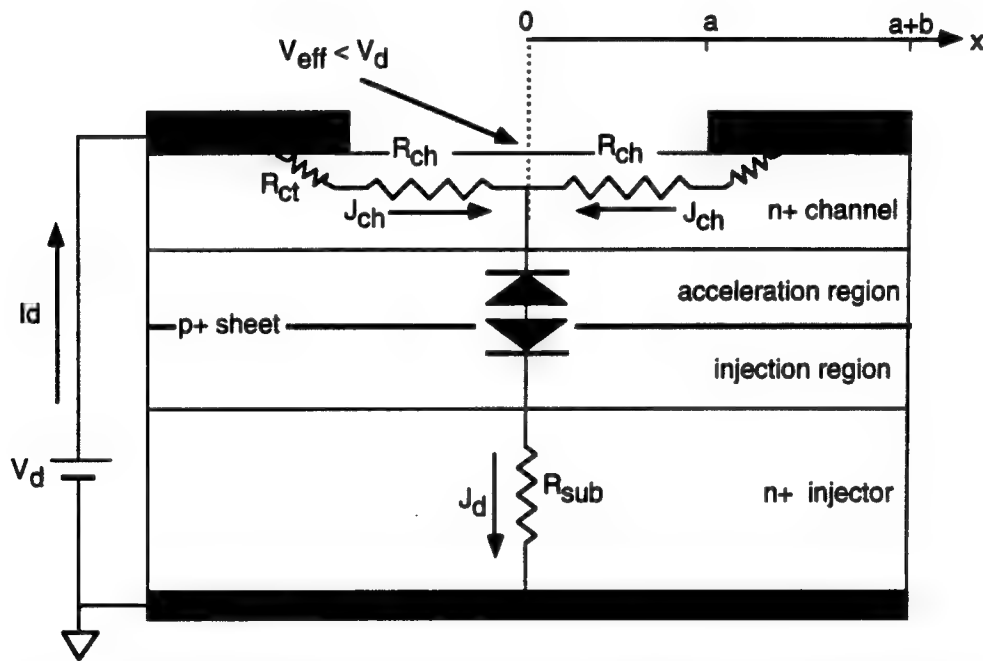


FIG. 10 A schematic diagram of the cross section of a PDBEE. Due to the existence of a thin channel, there is a lateral potential drop along the channel, making the center of the emission area less biased than the edges.

Emission characteristics of AlGaAs/GaAs PDBEEs

More work has been done on PDBEEs with $\text{Al}_{0.3}\text{Ga}_{0.7}\text{As}$ as the barrier material. Emitters and arrays with thinner surface channel layer and smaller emission areas have been designed in order to minimize both the scattering and current crowding. Table I shows the epitaxial structure of one of the best $\text{Al}_{0.3}\text{Ga}_{0.7}\text{As}$ PDBEEs grown by solid source MBE (Varian GEN-II). The thicknesses of the injection region, acceleration region and n-type channel layer are 150, 250 and 250\AA , respectively. The doping each layer is also listed in the table.

Table I Epitaxial structure of a $\text{Al}_{0.3}\text{Ga}_{0.7}\text{As}$ PDBEE (#9211-33)

Layer	Material	Thickness (\AA)	Dopant/ Doping
Contact layer	GaAs	20	Si/ $1 \times 10^{13} \text{ cm}^{-2}$
	GaAs	15	
	GaAs	15	Si/ $1 \times 10^{13} \text{ cm}^{-2}$
Channel	GaAs	80	Si/ $5 \times 10^{18} \text{ cm}^{-3}$
	$\text{Al}_{0.3}\text{Ga}_{0.7}\text{As}$	100	Si/ $1-5 \times 10^{18} \text{ cm}^{-3}$
			Si/ $1 \times 10^{13} \text{ cm}^{-2}$
	$\text{Al}_{0.3}\text{Ga}_{0.7}\text{As}$	20	
Barrier	$\text{Al}_{0.3}\text{Ga}_{0.7}\text{As}$	250	Be/ $2 \times 10^{13} \text{ cm}^{-2}$
	$\text{Al}_{0.3}\text{Ga}_{0.7}\text{As}$	150	
	graded AlGaAs	180	Si/ $1-5 \times 10^{18} \text{ cm}^{-3}$
Injector	GaAs	5000	Si/ $5 \times 10^{18} \text{ cm}^{-3}$

The cross section of a completed device is shown in Fig. 11, and Fig. 12 shows the SEM picture of the topology of PDBEEs. The emission surface was passivated with $(\text{NH}_4)_2\text{Sx}$ after fabrication, and then cleaned, *in situ*, by desorbing the sulfur overlayer in ultra-high vacuum. Cesium is then deposited onto emission surfaces at room temperature to lower the surface work function.

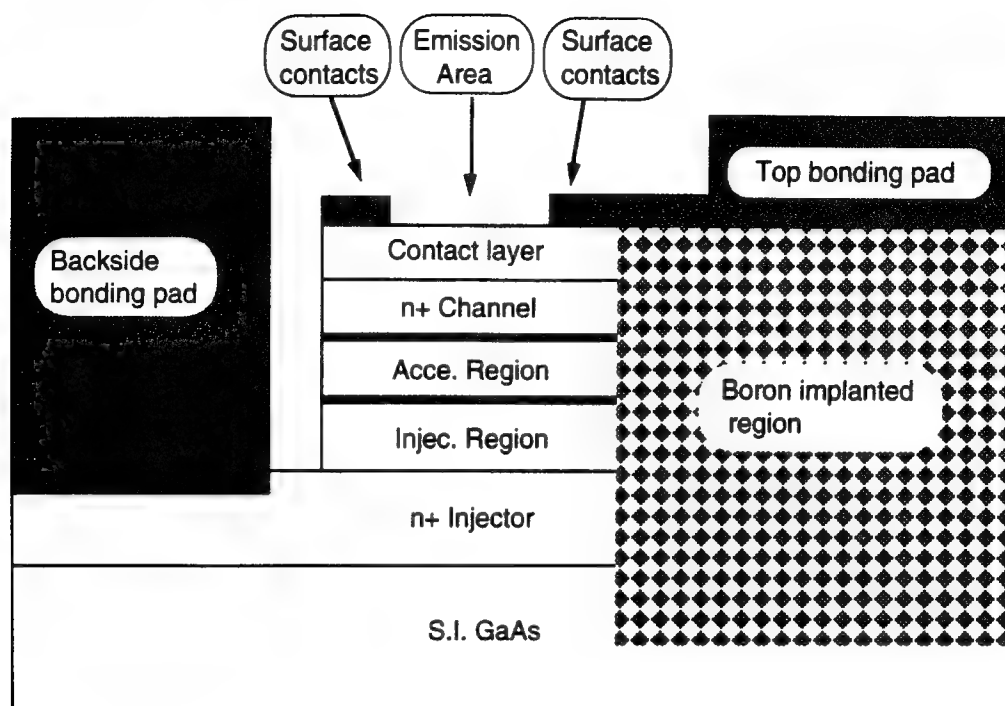


FIG. 11 Schematic cross section of a completed PDBEE.

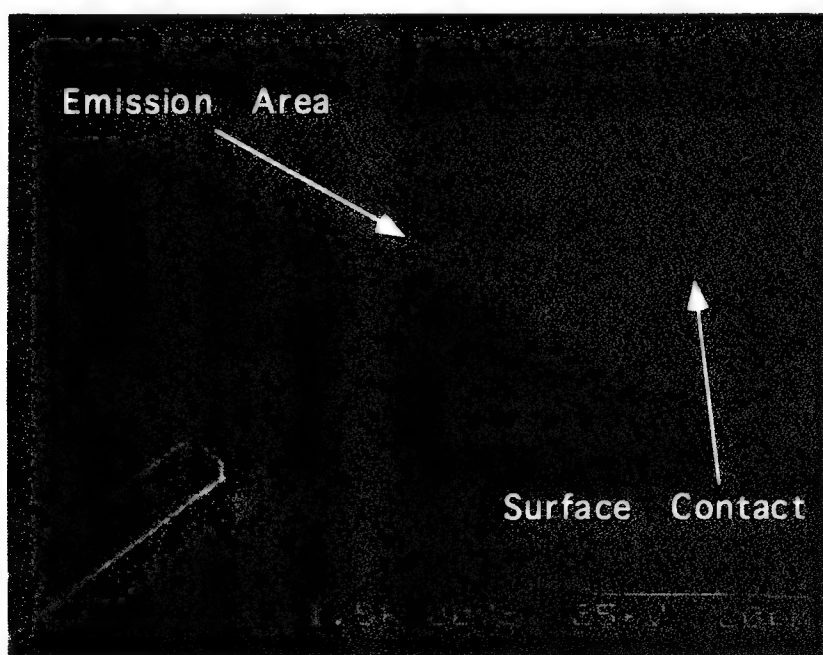


FIG. 12 SEM picture of the topology of PDBEEs

Fig. 13 shows the emission characteristics of the $\text{Al}_{0.3}\text{Ga}_{0.7}\text{As}/\text{GaAs}$ PDBEE with the epilayer structure shown in Table I. The peak emission efficiency is 4.2 % with an emission current density of 2.0 A/cm^2 . The maximum emission current density is about 5.8 A/cm^2 with an emission efficiency of 0.6 %.

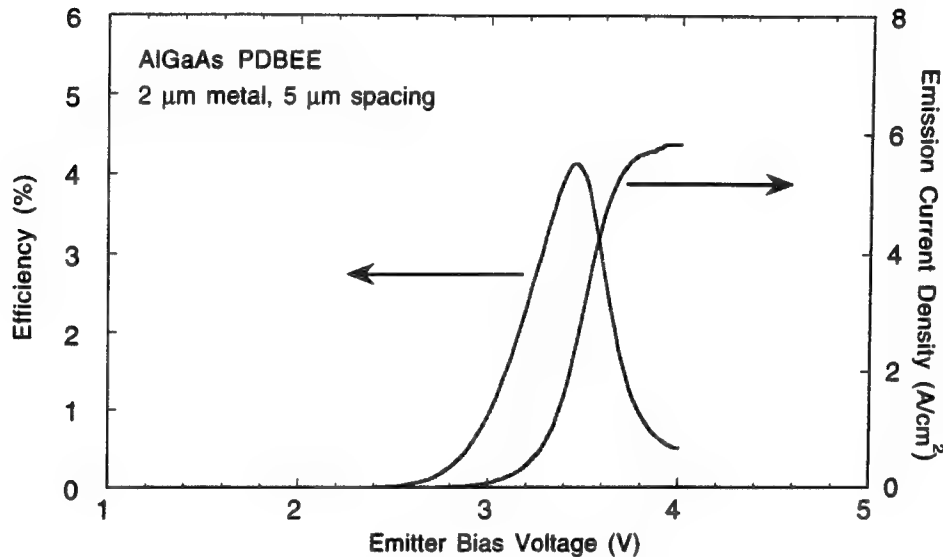


FIG. 13 Emission characteristics of a $\text{AlGaAs}/\text{GaAs}$ PDBEE.

Fig. 14 presents the emission current from the same $\text{AlGaAs}/\text{GaAs}$ PDBEE as a function of the anode bias at several emitter bias levels. The Ta anode is placed approximately 0.5 mm from the emission surface. The insert is an expanded view at a smaller current scale showing the onset of the emission. This figure is very similar to the I-V characteristics of a typical vacuum triode with a directly modulated emitter. The anode current saturates at about 60 volts for the highest emission current level.

Fig. 15 shows the emission characteristics of a $\text{AlGaAs}/\text{GaAs}$ PDBEE which was made from the same wafer as the one shown in Fig. 13, (the epilayer structure listed in Table I), but the channel layer within emission areas is thinned by etching away 50 \AA GaAs. The peak efficiency is about 6.7 % at an emission current density of 1 A/cm^2 , and the maximum emission current density is about 1.8 A/cm^2 at an emission efficiency of 3.5 %. Compared with the emitter shown in Fig. 13, the higher emission efficiency from this device is due to the 50 \AA thinner channel whereas the lower emission current density is due to more current crowding along a thinner channel.

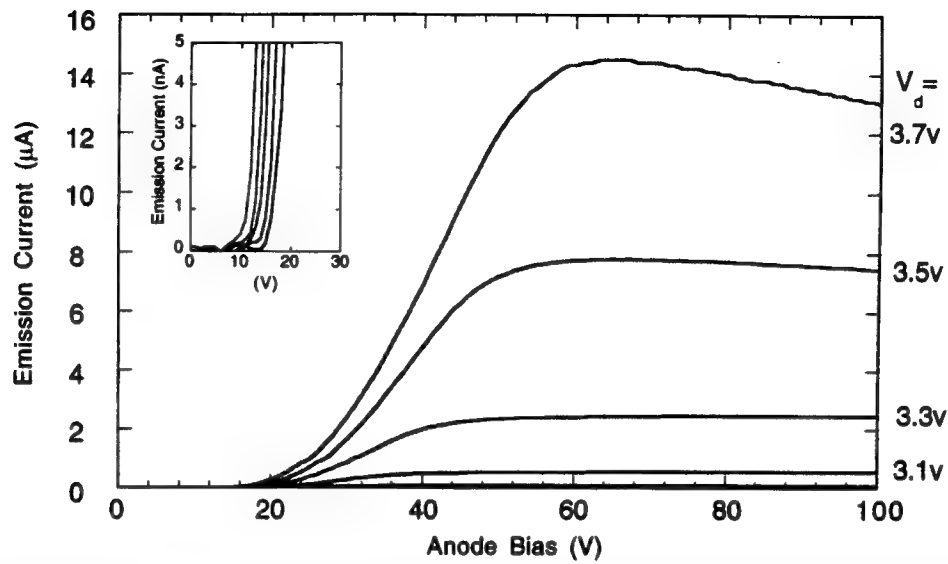


FIG. 14 Emission current vs. anode voltage at different emitter bias voltages as indicated in the figure. The anode bias is scanned from zero to 100 voltages. The insert is the blow-up at low current levels.

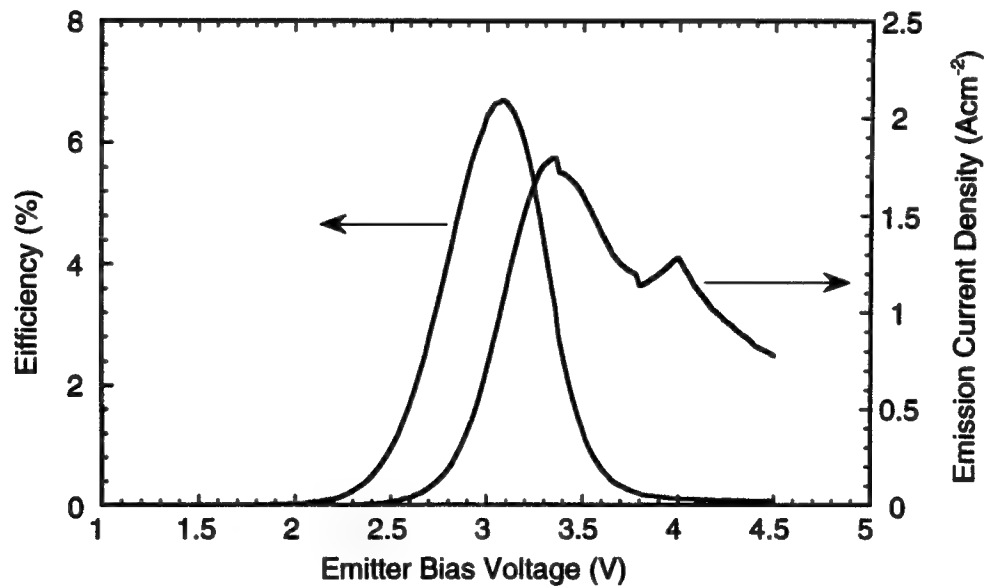


FIG. 15 Emission characteristics of a AlGaAs/GaAs PDBEE with the channel layer within the emission areas partially removed.

Although the current crowding degrades both the emission efficiency and emission current density, it has been shown that it affects the emission efficiency much less than emission current density. Therefore, although the device with the channel partially removed has a thinner channel and enhanced current crowding, the emission efficiency is still improved by 60 % because of reduced hot electron scattering.

In summary, planar electron emission has been demonstrated from semiconductor surfaces using AlGaAs/GaAs planar-doped-barrier structures. Emission efficiency of over 5 % and emission current density of over 5 A/cm² have been obtained from cesiated AlGaAs/GaAs PDBEEs.

As mentioned earlier, compared with solid state cathodes with different hot electron generation mechanisms, PDBEEs are majority carrier devices and the electrons are injected over the barrier by a forward biased p-i-n junction and accelerated by another reverse biased p-i-n junction. Therefore, high emission efficiency and high emission current density can be obtained at the same time. However, since it is difficult to apply a larger enough acceleration voltage across a thin region while maintaining the dominant current mechanism as thermionic emission over the barrier, the surface of AlGaAs/GaAs PDBEEs had to be cesiated to obtain measurable emission current. It has been long recognized that cesiated surfaces are not stable over the time so that the application of cesiated SSCs are limited.

In order to obtain electron emission from non-cesiated SSCs, it is necessary to heat electrons to kinetic energy level of about 5 eV within a region less than the hot electron mean free path. In this proposal, we propose non-cesiated SSCs made from GaN based materials.

Future Work: GaN based Non-cesium solid state cathodes

Based on the study of AlGaAs/GaAs PDBEEs, it can be concluded that materials with even larger band gap are necessary to suppress the band to band tunneling since it decreases drastically with increasing band gap. GaN has an energy band gap of about 3.4 eV. Fig. 16 presents the calculated tunneling current density across the acceleration region of both GaAs and GaN PDBEEs as a function of the acceleration voltage. Even with an acceleration region of only 100 Å, the tunneling current is essentially negligible.

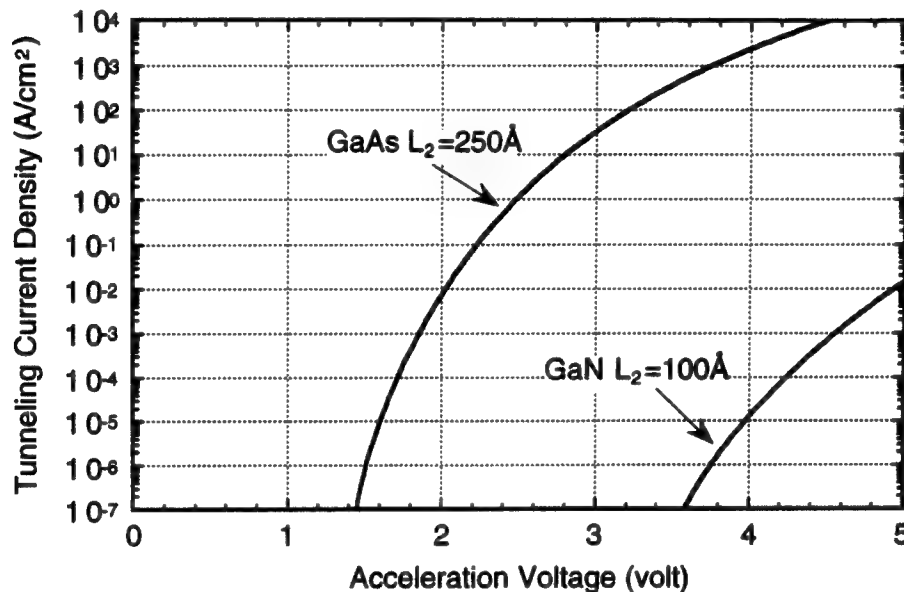


FIG. 16 Band to band tunneling vs.. acceleration voltage

As a result, a larger acceleration voltage can be applied across a thinner acceleration region with negligible tunneling contribution. This allows new approaches to achieve electron emission. The new approaches proposed here include (1) GaN based PDBEEs, and (2) AlN/GaN tunneling cathodes.

1. GaN based PDBEEs

As a continuous research on planar-doped-barrier electron emitters, we propose here GaN PDBEEs with two different terminating materials: (a) n-type GaN, and (b) metals.

(a) GaN terminated GaN PDBEEs

Future Work: GaN based Non-cesium solid state cathodes

Based on the study of AlGaAs/GaAs PDBEEs, it can be concluded that materials with even larger band gap are necessary to suppress the band to band tunneling since it decreases drastically with increasing band gap. GaN has an energy band gap of about 3.4 eV. Fig. 16 presents the calculated tunneling current density across the acceleration region of both GaAs and GaN PDBEEs as a function of the acceleration voltage. Even with an acceleration region of only 100 Å, the tunneling current is essentially negligible.

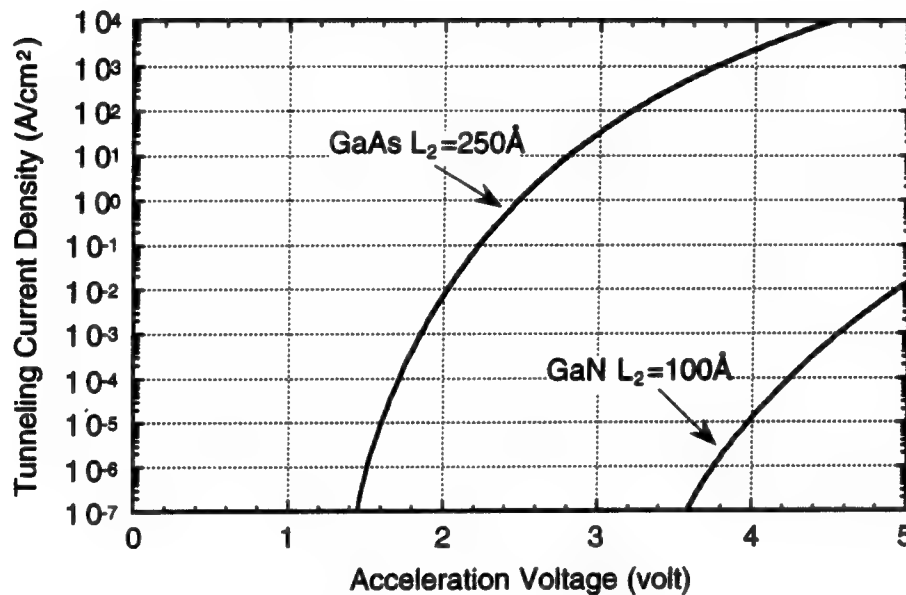


FIG. 16 Band to band tunneling vs.. acceleration voltage

As a result, a larger acceleration voltage can be applied across a thinner acceleration region with negligible tunneling contribution. This allows new approaches to achieve electron emission. The new approaches proposed here include (1) GaN based PDBEEs, and (2) AlN/GaN tunneling cathodes.

1. GaN based PDBEEs

As a continuous research on planar-doped-barrier electron emitters, we propose here GaN PDBEEs with two different terminating materials: (a) n-type GaN, and (b) metals.

(a) GaN terminated GaN PDBEEs

Fig. 17 presents the proposed GaN PDBEEs with n-type GaN as the terminating top layer. This structure is the exact extension of AlGaAs/GaAs PDBEEs. Due to the large band gap of GaN, the band to band tunneling is greatly reduced. Therefore, a large acceleration voltage (>5 volts) can be applied across a very thin acceleration region ($<100\text{\AA}$) while the dominant current mechanism remains the thermionic emission over the barrier.

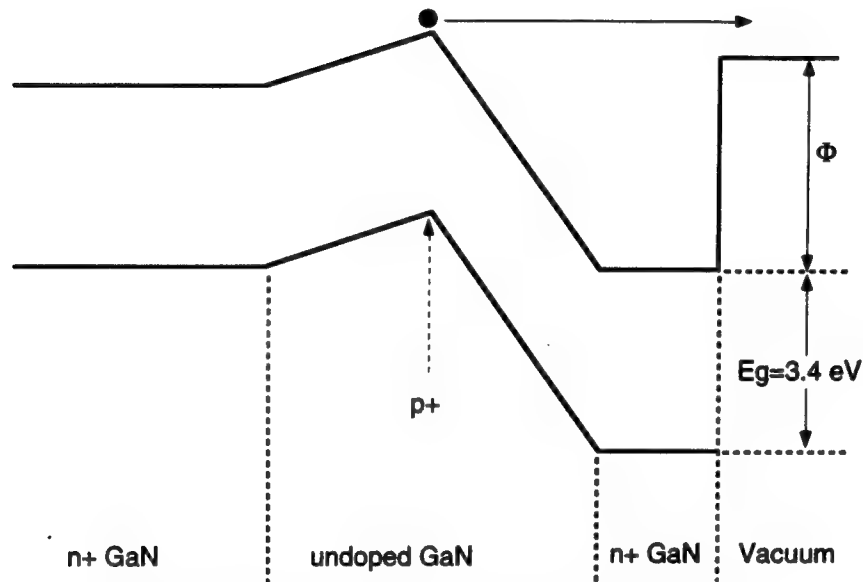


FIG. 17 Schematic energy band diagram of a GaN PDBEE

The channel layer of the GaN PDBEEs is n-type GaN. As discussed earlier, a conducting channel is necessary to drain the electrons reflected at the surface barrier. Since the channel layer has to be very thin to minimize hot electron scattering, the injection current is not uniform within an emission area due to the current crowding. As a widegap material, GaN has a lower electrical conductivity than GaAs (at least one order of magnitude lower). Therefore, a thicker GaN channel is necessary to minimize the current crowding. An alternative approach of the structure shown in Fig. 17, GaN PDBEEs with metals as the top terminating layer (subsequently called as M/GaN PDBEEs) are will also be studied as detailed below.

(b) Metal terminated GaN PDBEEs (M/GaN PDBEEs)

Fig. 18 presents the schematic energy band diagram of a M/GaN PDBEE. In this structure, the top n-type GaN channel layer is replaced by a very thin layer of metal (e.g.

Hf). Electron injection, acceleration and emission mechanism in M/GaN PDBEEs are the same as in a GaN PDBEE. There are two major advantages of M/GaN PDBEEs over GaN PDBEEs. (1) Most metals have an electron conductivity of 2~3 orders of magnitude

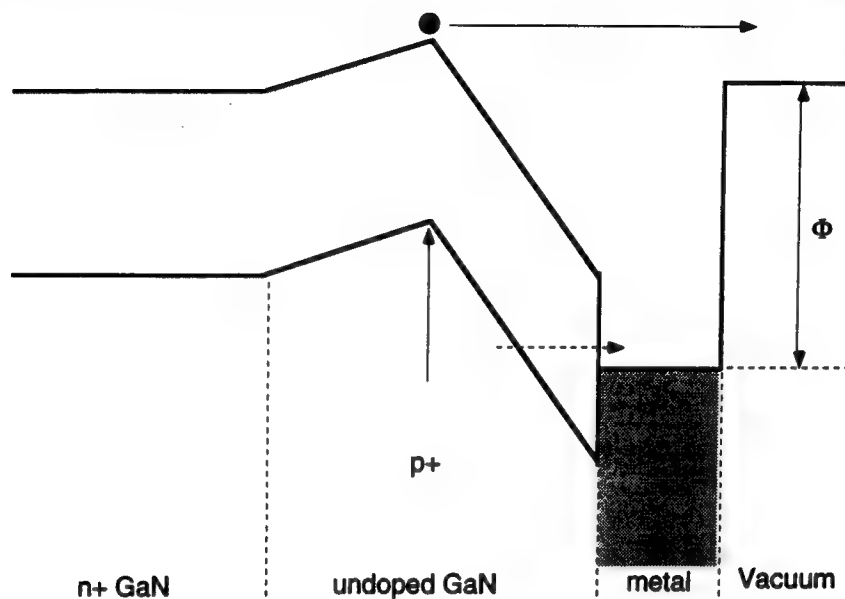


FIG. 18 Schematic band diagram of a M/GaN PDBEE. The dashed arrow shows the tunneling of electrons from the valence band to the interface states between the metal and GaN acceleration region or to states above the Fermi level within the metal.

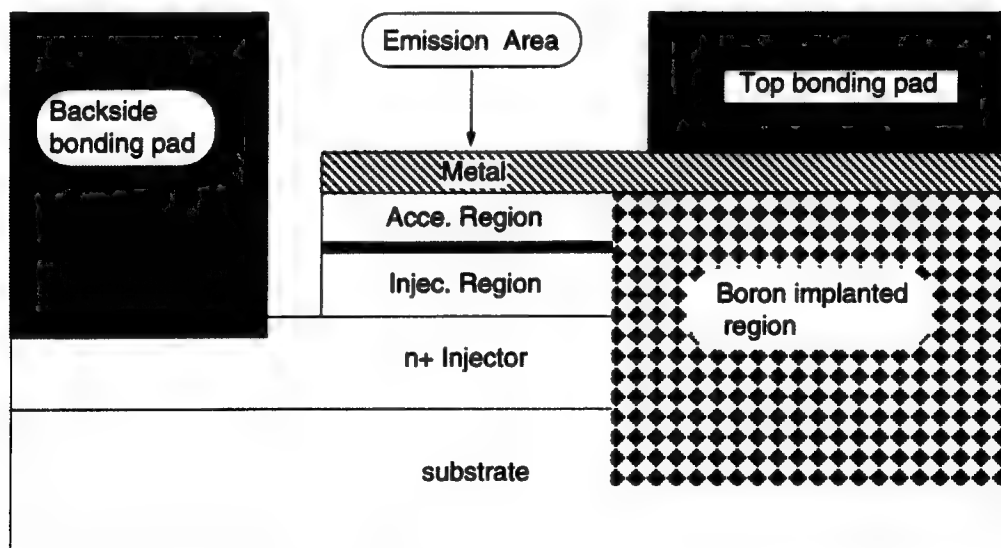
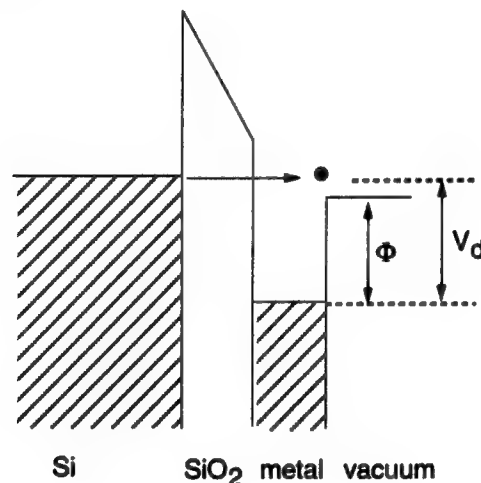


FIG. 19 Cross section of a M/GaN PDBEE.

higher than semiconductors. Therefore, the current crowding along the channel will be greatly reduced even with a thinner channel. (2) The top metal layer which serves as the contact layer also overlays the emission area as shown in Fig. 19. This eliminates the parasitic current which directly flows towards the surface contacts as shown in Fig. 11, and therefore, the emission efficiency will be greatly improved.

2 AlN/GaN tunneling electron emitters

Another possible structure to generate hot electrons is the tunneling structure which was first proposed by Mead in 1960. Very recently, a group at Tohoku University, Japan, demonstrated electron emission from the Al/SiO₂/Si MOS structure shown in Fig. 20. An emission efficiency of 0.7 % was reported from the non-cesium MOS tunneling structure. However, the emission current density is low and the deterioration of the oxide at high field results in poor stability.



We propose here a tunneling electron emitter based on AlN/GaN. A schematic band diagram is shown in Fig. 21. AlN has an energy band gap of 6.2 eV and can grown on GaN with negligible lattice mismatch. The structure shown in Fig. 21 is composed of a thin layer of undoped AlN ($\sim 50\text{\AA}$) sandwiched between a n^+ GaN layer and a thin film of metal ($< 100\text{\AA}$). The mechanism of this device is exactly the same as that of MOS tunneling emitters. When a bias is applied between the n^+ GaN and top metal layer, most of the bias will be across the AlN layer, since the GaN layer is heavily n-type doped.

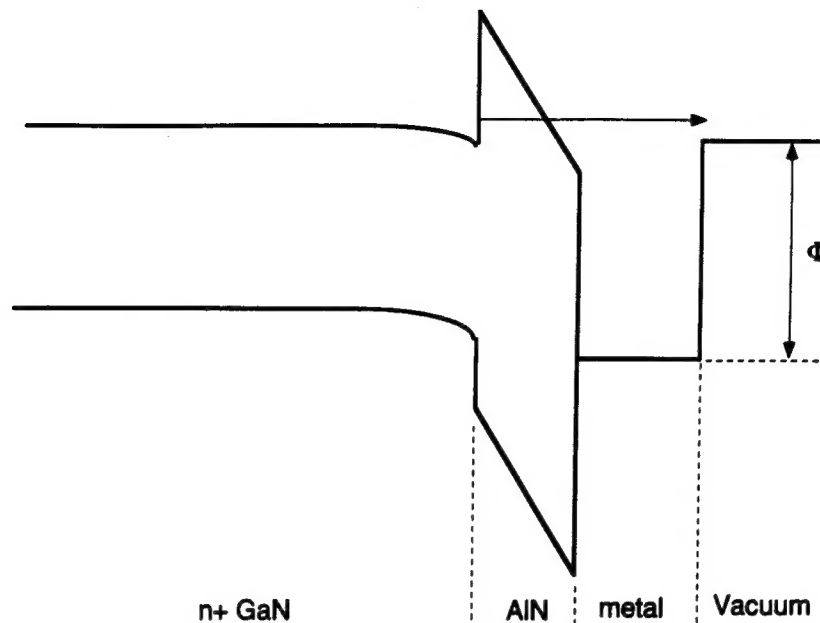


FIG. 21 A schematic band diagram of AlN/GaN tunneling emitters

Because of a large ΔE_c between GaN and AlN, estimated between 1.2~1.8 eV, the current across this AlN/GaN structure will be dominated by the tunneling across the AlN layer, if the AlN layer is thin enough allowing substantial tunneling. *Unlike the Si-SiO₂ MOS structure in which SiO₂ is an amorphous layer, AlN can be lattice matched grown on GaN. Therefore, AlN layer is expected to be more stable than SiO₂ under high fields.*

The AlN/GaN tunneling emitter has a very simple structure. With the rapid development of today's nitride growth technology, high quality doped GaN and undoped AlN can be successfully grown on SiC or sapphire substrates. The hot electron generation mechanism of the AlN/GaN tunneling emitter is similar to that of field emitters. Both are based on the tunneling of electrons across a barrier under high fields. Therefore AlN/GaN tunneling emitters can be described as planar field emitters. The large band gap of AlN and single crystal quality promise stable high emission current density and high emission efficiency. The electron energy distribution obtained from AlN/GaN tunneling emitters is also expected narrow due to the tunneling nature. Resonant tunneling emitters can also be readily incorporated to reduce the electron energy distribution and enhance emission current density.

Appendix I Papers and conference presentations generated by this research

1. W.N. Jiang, D.J. Holcombe, M.M. Hashemi and U.K. Mishra, "InGaAs/GaAs Planar Doped Barrier Electron Emitters", Technical Digest, 50th Annual Device Research Conference, Cambridge, MA, USA, 22-24, June 1992
IEEE Trans. on Electron Devices, **ED-39**, 2649 (1992)
2. W.N. Jiang and U.K. Mishra, "A Novel Electron Emitter with AlGaAs Planar Doped Barrier", Technical Digest, IEDM'92, San Francisco, CA, Dec. 14-16, 1992, page. 985
3. W.N. Jiang, D.J. Holcombe, M.M. Hashemi, and U.K. Mishra, "GaAs Planar Doped Barrier Vacuum Microelectronic Electron Emitters", IEEE Electron Device Letters, **14**, 143 (1993)
4. W.N. Jiang, U.K. Mishra, "Current Flow Mechanisms In GaAs Planar-Doped-Barrier Diodes With High Built-in Fields", J. Appl. Phys., **74**, 5569 (1993)
5. W.N. Jiang, U.K. Mishra, "1 % efficiency $\text{Al}_{0.3}\text{Ga}_{0.7}\text{As}$ /GaAs Planar-Doped-barrier Electron Emitters", Electron. Lett., **29**, 1997 (1993)
6. W.N. Jiang, U.K. Mishra, "Study Of The I-V Characteristics Of Planar-Doped-Barrier Electron Emitters (PDBEEs)",
J. Vac. Sci. Technol., **B12**, 795 (1994)
7. U.K. Mishra and W.N. Jiang, "Planar Cold Cathodes", IEEE Cornell Conference, 1993
8. W.N. Jiang, R. D. Underwood and U.K. Mishra, " $\text{Al}_{0.3}\text{Ga}_{0.7}\text{As}$ /GaAs Planar-Doped-barrier Electron Emitters", presented at 1994 Tri-Service/NASA Cathode Workshop, Cleveland, Ohio, March 29-31, 1994

Appendix II Ph.D thesis generated by this research

Wei-Nan Jiang, "AlGaAs/GaAs Planar-Doped-Barrier Electron Emitters: Design, Fabrication, and Characterization", see attached documents.

References

- ¹ for example, C. A. Spindt, I. Brodie, L. Humphrey, and E. R. Westerberg, "Physical properties of thin film field emission emitters", J. Appl. Phys. **47**, 5248 (1976)
- ² for example, A. I. Akinwanda, P. E. Banhahn, H. F. Gray, T. R. Ohnstein, and J. O. Holmen, "Mamo-metr scale thin film-edge emitte devices with high current density characteristics", in Technical Digest of IEDM, 1992 p. 367; and
J. Itoh, K. Ushiki, and K. Tsuburaya, "Fabrication of lateral triode with comb-shaoed field-emitter arrays", in International Vacuum Microelectronic Conference (IVMC), Newport, RI, July 12-15, 1993, p.99
- ³ C. A. Spindt, C. E. Holland, A. Rosengreen, and I. Brodie, "Field-emitter-array development for high-frequency operation", J. Vac. Sci. Technol. B **11**(2), 468 (1993)
- ⁴ planar emitters
- ⁵ for example, G. G. P. van Gorkom and A.M.E. Hoeberechts, "Silicon cold cathodes", Phillips Tech. Rev. **43**, 49 (1987)
- ⁶ W.N. Jiang, D.J. Holcombe, M.M. Hashemi, and U.K. Mishra, "GaAs Planar Doped Barrier Vacuum Microelectronic Electron Emitters", IEEE Electron Device Letters, **14**, 143 (1993)
- ⁷ K. Yokoo, H. Tanaka, S. Sato, J. Murota, and S. Ono, "Emission characteristics of metal-oxide-semiconductor electron tunneling cathode", J. Vac. Sci. Technol. **B11**(2), 429 (1993)